Published in final edited form as:
Heart Rhythm. 2012 February ; 9(2): 275–282. doi:10.1016/j.hrthm.2011.09.066.

Arrhythmia formation in subclinical ("silent") long QT syndrome requires multiple insults: Quantitative mechanistic study using the *KCNQ1* mutation Q357R as example

Thomas O'Hara, PhD and **Yoram Rudy, PhD, FHRS**
Department of Biomedical Engineering, Cardiac Bioelectricity and Arrhythmia Center, Washington University in St. Louis, St. Louis, Missouri

Abstract

BACKGROUND—In subclinical or silent long QT syndrome, the QT interval is normal under basal conditions. The hypothesis that insults to the repolarization reserve may cause arrhythmias in silent mutation carriers but not in noncarriers has been proposed as a general principle, yet crucial aspects remain descriptive, lacking quantification.

OBJECTIVE—To utilize accurate mathematical models of the human action potential and β-adrenergic stimulation to quantitatively investigate arrhythmia-formation mechanisms peculiar to silent long QT syndrome, using mutation Q357R in *KCNQ1* (α subunit of slow-delayed rectifier I_{Ks}) as a paradigm.

METHODS—Markov models were formulated to account for altered I_{Ks} kinetics in Q357R compared with wild type and introduced into a detailed model of the human ventricular myocyte action potential.

RESULTS—Dominant negative loss of I_{Ks} available reserve accurately represents Q357R. Action potential prolongation with mutant I_{Ks} was minimal, reproducing the silent phenotype. Partial block of rapid delayed rectifier current (I_{Kr}) was needed in addition to fast pacing and isoproterenol application to cause early after-depolarizations (EADs) in epicardial cells with mutant I_{Ks}, but this did not produce EADs in wild type. Reduced channel expression at the membrane, not I_{Ks} kinetic differences, caused EADs in the silent mutant. With mutant I_{Ks}, isoproterenol plus partial I_{Kr} block resulted in dramatic QT prolongation in the pseudo-electrocardiogram and EADs formed without I_{Kr} block in mid-myocardial cells during simulated exercise onset.

CONCLUSION—Multiple severe insults are needed to evince an arrhythmic phenotype in silent mutation Q357R. Reduced membrane I_{Ks} expression, not kinetic changes, underlies the arrhythmic phenotype.

Keywords

Action potential; β-Adrenergic stimulation; Computational models; Electrophysiology; Isoproterenol; Long-QT syndrome; Repolarization reserve; Silent mutation

Address for reprints and correspondence: Dr Yoram Rudy, PhD, Department of Biomedical Engineering, Cardiac Bioelectricity and Arrhythmia Center, Washington University in Saint Louis, Campus Box 1097, 290 Whitaker Hall, One Brookings Drive, Saint Louis, MO 63130. rudy@wustl.edu..

Appendix Supplementary data Supplementary data associated with this article can be found, in the online version, at doi:10.1016/j.hrthm. 2011.09.066.

Introduction

Long QT syndrome (LQTS) can cause cardiac arrhythmia and sudden death in the absence of structural heart disease.[1] LQTS affects as many as 1 in 2000 among Caucasians.[2] The most common form of LQTS is type 1 (LQT1), with *KCNQ1* as the locus of mutations,[3] a gene that transcribes the Kv7.1 protein, forming the α subunit of the repolarizing slow delayed rectifier K^+ current I_{Ks}.

Although LQT1 is less deadly than other forms of LQTS, lethality increases considerably with emotional/physical stress or exercise, conditions associated with β-adrenergic stimulation and fast heart rate.[4] These conditions and also certain drug effects (eg, block of rapid-delayed rectifier I_{Kr}) increase the arrhythmia risk by challenging the genetically compromised repolarization reserve due to LQT1 mutation.[5] It has been conceptualized that physiological or external insults to the repolarization reserve, individually innocuous, combine synergistically to create arrhythmia substrates and cause fatal arrhythmias. As stated by A. Wilde, “a double hit hurts more.”[6]

An enigmatic case of subclinical or “silent”[7] LQT1 was identified, missense mutation Q357R near the S6–C-terminal junction of Kv7.1 (Boulet et al[8]). Q357R was discovered in a 40-year-old female proband with a history of syncope, but with the corrected QT interval within the normal range (430 ms).[9] The absence of electrocardiogram (ECG) phenotype associated with this silent mutation obscures the connection between phenotype and arrhythmia. Exhaustive measurements by Boulet et al[8] showed that Q357R is characterized by partial loss of I_{Ks} function, a current that is of small magnitude in the human ventricle under basal conditions.

Observations of Boulet et al at the level of I_{Ks} current suggest only a vague possibility of minor action potential (AP) repolarization changes and marginally increased arrhythmia risk for this silent mutation carrier. Thus, several clinical questions are raised: Is it reasonable to suspect that the silent mutation was in fact the cause of syncope in the proband? That is, can known LQT1 insults (emotional/physical stress or exercise) account for arrhythmia formation in this case of silent LQT1? Moreover, is the consequence of the silent mutation so mild that these insults affect mutant and wild-type (WT) I_{Ks} similarly, causing a similar phenotype? If so, the silent mutation may not be the cause of syncope. Finding answers to these questions requires quantification beyond qualitative predictions. Motivated to investigate and explain the possibility of arrhythmia formation in humans with silent LQTS, we investigated Q357R as an instructive paradigm, using newly available, quantitatively accurate mathematical models.

Methods

Using experiments from Boulet et al,[8] human I_{Ks} models for WT and Q357R were developed. AP simulations were conducted by using the O'Hara Rudy dynamic human ventricular action potential model (ORd).[10] Simulations were performed in epicardial (epi) and mid-myocardial (M) cells and in a transmural wedge model from which the pseudo-ECG was computed[11] mimicking experiments.[12] Further details are given in the Supplement. Simulation results for APs or pseudo-ECGs were always preceded by a train of pacing that is not shown. For plotting purposes, time is reset to begin at t = 0, though the true simulation time is much larger.

To determine β-adrenergic stimulation effects on I_{Ks} and resulting changes to its role in the AP, we adapted the model by Heijman et al,[13] including signaling cascade from isoproterenol (ISO) application to compartmentalized protein kinase A concentration and

fractional phosphorylation of targets. Equations, validation, and details are given in the Supplement (Supplement Figures S1 and S2).

Unless otherwise stated, black, dashed black, and gray lines are simulation results for WT, Q357R, and the heterozygous (het) case, respectively. Current symbols: fast Na^+ (I_{Na}), L-type Ca^{2+} (I_{CaL}), Na^+/K^+ ATPase (I_{NaK}), ultrarapid K^+ (I_{Kur}, represented by K^+ background, I_{Kb} in ORd).

Results

Q357R I_{Ks} kinetics and behavior

WT I_{Ks} was represented by the Markov model developed by Silva and Rudy[14] shown in Figure 1A, left. The activation of WT channels involves slow transitions from left to right in zone 2 of deep closed states, followed by rapid transitions only, from top to bottom, in zone 1 of closed states. Accumulation in zone 1 states, which are kinetically near the open states, provides an available reserve[14] of channels that can activate rapidly. By contrast, we hypothesized that Q357R mutant channels do not develop an available reserve. That is, Q357R channels activate with 2 identical slow zone 2–like transitions between all closed states. To implement this, we replaced top-to-bottom transition rates ("g" and "d" in WT) with the left-to-right transition rates ("a" and "b" in WT, slightly modified to "A" and "B" in Q357R). In addition, compared with WT, the Q357R model includes depolarization-directed shifts in the voltage dependence of transition rates. Conductance was reduced by 50% to represent the observed lower expression at the membrane.

Boulet et al created the het case by injecting cells with equal amounts of Q357R and WT cDNA. There are 6 permutations of WT and Q357R subunit pairings that can form channel tetramers (Figure 1B). We tested whether dominant negative mutant behavior could account for het results. That is, the model assumes that WT and Q357R tetramer assembly is random (but lumping together degenerate cases); presence of ≥1 Q357R subunit(s) slows gating for the entire channel, and presence of ≥1 Q357R subunit(s) attenuates membrane expression. These assumptions (schematized in Figure 1B) allowed us to develop and test a putative model for average het channel behavior. Accordingly, het current calculation was the weighted average of computed Q357R and WT currents, added together in a 5:1 mixture. We tested whether allowing only subsets of all heterotetramer permutations would affect the comparison with experiments. The model that allowed all permutations provided the best overall fit to the experimental data (Supplement Figure S3).

Using the assumptions described, models reproduced the kinetics of the experimentally recorded Q357R and het currents compared with WT (Figure 2). Specifically, for mutant current simulation compared with WT, the (1) steady-state activation was shifted to more depolarized potentials, (2) activation rate was slowed, (3) deactivation rate was unaffected, and (4) tail current was reduced. The correspondence between simulations and experiments supports the hypothesis that Q357R can be considered as dominant negative loss of available reserve.

Model design was hypothesis driven, guided by previous simulations[14] and experimental observations.[8,15] We did not consider other models of the mutant channel. Five free parameters were needed to capture essential behaviors. Parameter values were determined by fitting the simulated kinetics to experimental data. Parameter sensitivity analysis is provided in Supplement Figure S4.

Phenotype is silent under basal conditions

We tested the effect of replacing WT with Q357R or het I_{Ks} in different cell types at normal heart rate under basal conditions (cycle length [CL] = 1000 ms, no ISO, Figure 3). In epi cells, Q357R and het had very little effect on the AP duration (APD). Prolongation was 14 and 12 ms, respec tively. For M cells, it was 30 and 23 ms, respectively. These are small increases (≤8.5% increase), though larger than those for epi cells (≤6.0% increase). Such minor AP prolongation under basal conditions reproduces the silent phenotype. Note that I_{Ks} was reduced significantly by the mutation, though it is relatively small to begin with in WT.

Somewhat surprisingly, after many beats of pacing (t = 0 in Figure 3 is the start of the final paced AP), occupancy in rapidly activating zone 1 states of I_{Ks} was actually higher for Q357R compared with WT in both epi and M cells (Figure 3, bottom); that is, zone 1 accumulation[16] during pacing was greater in the mutant (explained later).

Multiple insults to the repolarization reserve cause early afterdepolarizations in the silent mutant, not in WT

In Figure 4, insults to the repolarization reserve, representing known arrhythmia triggers in LQT1, were added sequentially in epi cell simulations. They included (1) fast pacing (CL = 300 ms), (2) β-adrenergic stimulation (1 μM ISO), and (3) partial I_{Kr} block (30%). With fast pacing, Q357R and het prolonged the AP by only negligible amounts (8 and 7 ms, respectively). Note that the prolongation was less than that observed at the slower resting heart rate (CL = 1000 ms, far left column, 14 and 12 ms prolongation for Q357R and het, respectively). This is typical of the LQT1 clinical phenotype, where prolongation is more severe at slower rates, though arrhythmic events are associated with fast heart rates.[1,4] When ISO was added to fast pacing, the APD was increased by 27 and 21 ms for Q357R and het respectively, relative to WT at basal conditions (CL = 1000 ms). The increase was 15 ms (Q357R) and 10 ms (het) compared with that without ISO at CL = 300 ms. It was due to a larger inward I_{CaL} that was not countered sufficiently by an increase in the mutation-compromised I_{Ks}. By contrast, ISO slightly decreased the WT APD (4 ms, shown in Supplement Figure S2).

Adding a partial I_{Kr} block to ISO at a fast rate caused WT epi APD to increase by 31 ms. For Q357R and het, epi APD was severely prolonged under these conditions; extended time at depolarized plateau voltages allowed I_{CaL} reactivation, triggering early afterdepolarizations (EADs) (mechanism shown previously[10]). Supplement Figure S5 shows that no EADs formed when insults were applied individually (not layered sequentially).

In M cells, with the first insult alone (fast pacing), the Q357R and het I_{Ks} changes had a strong effect on the AP (Supplement Figure S6).

I_{Ks} gating kinetic changes in the silent mutant were not responsible for EADs

The I_{Ks} zoom inset in Figure 4 (third row) shows that mutant I_{Ks} was actually larger than WT I_{Ks} for the first approximately 40 ms of the AP. However, mutant current amplitude was approximately half that of WT once peak values were reached during the critical phase 3 of the AP, when repolarizing current can effectively shorten the APD. Pacing for many beats caused accumulation in zone 1 for both WT and Q357R, as anticipated[14,16] (Figures 3 and 4, bottom rows). However, as mentioned earlier, zone 1 accumulation was greater for Q357R than for WT, explaining the appearance of early current in the mutant. Greater zone 1 accumulation with pacing was due to slowed “deep deactivation” in the mutant, defined as the transition from shallow zone 1 closed states to deep zone 2 closed states (see Supplement Figure S7; a detailed explanation is provided in the figure caption). This result is a model

prediction, not tested experimentally by Boulet et al, whose protocols did not include the response of I_{Ks} to pacing.

Although interesting, the I_{Ks} kinetic differences associated with the Q357R mutation were not responsible for EAD formation, as described below. To test whether altered gating kinetics of Q357R might have contributed to EAD generation after multiple insults, component mutants were investigated: one with altered conductance alone (type A) and another with altered gating kinetics alone (type B). Qualitative results for component mutant type A were the same as for Q357R and het (Figure 5). The AP was prolonged, and then EADs formed after the insults were layered. Although mutant type B showed noticeable AP prolongation compared with WT after insults, EADs did not form. These results signify that the more arrhythmic consequence of Q357R is due to reduced channel expression at the membrane, represented by reduced channel conductance. Kinetic differences were not a determining factor in EAD formation.

Heterogeneous transmural wedge simulations

To determine how the Q357R mutation affects repolarization in the more realistic context of heterogeneous tissue, we performed transmural wedge (pseudo-ECG) simulations (Figure 6). Under basal conditions, the silent mutation barely affected the QT interval (15 and 13 ms longer for Q357R and het, respectively, compared with WT). With ISO application, prolongation was 24 and 23 ms for Q357R and het relative to WT, and T-wave amplitude increased. With I_{Kr} block added, QT prolongation relative to WT became severe for Q357R and het (>80 ms). ISO plus I_{Kr} block-induced prolongation for Q357R and het was nearly twice (1.8-fold) that for WT. Dispersion of repolarization, measured as T-peak to T-end duration, was 2-fold larger for the mutant cases. However, the WT T-wave was also markedly affected by these conditions.

Onset of emotional/physical stress or exercise

Arrhythmia in LQT1 occurs during transition to a state of emotional/physical stress (eg, exercise onset[4] or diving into a pool[1]). To simulate this transient scenario, we accelerated the pacing rate and applied a bolus of ISO (using the more mutation-sensitive M cell, Figure 7). The pacing rate was doubled, from CL = 1000 to 500 ms, in a graded fashion over approximately 7 seconds, as observed in human subjects during exercise onset.[17] For I_{CaL}, the fraction of channels phosphorylated by protein kinase A increased more rapidly than for I_{Ks} (validated previously[13]). Eventually, the resulting imbalance between inward and outward current ISO responses led to pronounced EADs, even without I_{Kr} block, in the silent mutant cases.

Other exercise-onset simulation results are worth mentioning. With the addition of 30% I_{Kr} block, EADs appeared in WT as well as Q357R and het in M cells. In epi cells, EADs appeared in Q357R and het only with 30% I_{Kr} block. However, under these conditions, they also appeared in WT.

Discussion

As shown by Jost et al,[18] the small-magnitude human I_{Ks} is augmentable, helping to shorten the AP as rate increases and terminate the AP when the repolarization reserve is compromised. Silva and Rudy[14] simulations showed that I_{Ks} augmentation can overcome an EAD due to I_{Kr} block and restore normal repolarization. These concepts explain how I_{Ks} loss of function leads to arrhythmia formation in patients with LQT1. However, with silent mutant Q357R, the phenotype is so mild that the applicability of these concepts is suspect. Is it plausible to assume that the silent mutation is the sole cause of arrhythmia? To answer this

question, rigorous quantitative analysis is needed. In guinea pig simulations, arrhythmic Q357R and het phenotypes were revealed under basal conditions alone, without any repolarization reserve insults (Supplement Figure S8). This consequence of species-dependent ionic profiles (large I_{Ks} in guinea pig) highlights the fact that quantitative accuracy is paramount when investigating silent mutations where arrhythmia formation is marginal.

Because of the mild phenotype, multiple insults to the repolarization reserve were required to reveal the abnormal behavior of the silent mutation compared with WT in humans. Fast pacing and ISO application alone substantially prolonged the APD (LQT phenotype) in this particular mutation, but the external factor of partial I_{Kr} block was needed to cause EADs in epi cells. In M cells during exercise onset, EADs formed without I_{Kr} block. These results are consistent with the accepted dogma for arrhythmia formation in LQT1. Relatively simple computer models helped develop these basic concepts. However, silent mutation effects are subtle and demand more sophisticated models for quantitative accuracy. The new simulations presented here showed that (1) separate insults are insufficient to differentiate silent mutant phenotype from WT (multiple insults are needed) and (2) multiple severe insults to the repolarization reserve may also affect WT. Therefore, a silent mutation must be investigated quantitatively to determine whether the mutation alone is indeed responsible for arrhythmia formation; the simulation results suggest that it may not be for Q357R.

Note that when EADs formed in silent mutant Q357R and in het, the WT was not unaffected. That is, multiple insults caused minor voltage deflections even in WT. If the final insult of partial I_{Kr} block was increased from 30% to 40%, EADs appeared in epi cells from WT as well (not shown). Also, during the characteristic arrhythmogenic LQT1 challenge of exercise onset, it was difficult to find conditions that revealed hidden arrhythmia propensity in silent mutant cases without also affecting WT behavior. The possibility of EAD generation in the WT model was validated previously[10] based on experiments showing EAD formation after nearly complete I_{Kr} block in slowly paced nonfailing isolated human ventricular myocytes.[19] However, in the intact heart, cells are electrically loaded and EAD formation is less likely. Taken together, the results cast doubt as to whether the silent mutation alone sufficiently explains syncope in the Q357R proband.

Dominant negative loss of available reserve

Missense mutation Q357R is an exchange of neutral glutamine for positively charged arginine at the junction between S6 and the C-terminus. Boulet et al's[8] experiments showed that because of the influence of the positive arginine, voltage-dependent gating was affected. We speculate that placement of mutant arginine adjacent to the positive–negative charge interactions between S4 and S2 segments[20] could disrupt gating. However, in the absence of further experimental analysis based on structural detail, it remains unclear how this might amount to the observed slowing of activation.

Boulet et al[8] were not able to determine whether Q357R reduced membrane expression because of trafficking or assembly abnormalities. Simulations involved lumping together degenerate tetramer assemblies, which could reflect assembly abnormalities. Thus, our analysis cannot determine that Q357R-reduced membrane expression could be due to impaired trafficking alone. Additional experiments are needed to clarify this issue.

Limitations

The effects of β-adrenergic stimulation were validated on a target-by-target basis by using the ORd. The overall result of β-adrenergic stimulation on the AP and APD restitution are in agreement with nonfailing human ventricular measurements (Supplement Figures S1 and

S2). However, the experimental data set available for β-adrenergic effects on target proteins is nearly all from experiments performed in nonhuman mammals (dog), adapted here for humans.

Data are not available that compare the effects of β-adrenergic stimulation on Q357R versus WT. It is possible that differential effects exist. However, the simulations assume that the influence of ISO application was identical in both. Inherent gating differences could have but in fact did not cause different functional consequences of ISO application; the ISO-induced percentage increase in the charge carried by I_{Ks} during an AP was the same for WT, Q357R, and het (not shown). Thus, simulations predict that ISO application does not elevate EAD propensity in the silent mutant more than for WT. Moreover, the binding site for the β-adrenergic signaling complex (near residue 589)[21] is distal to the mutation site.

The pseudo-ECG generated by a 1D transmural fiber is related to but not equated with the clinical ECG, where the QT interval reflects the time between the earliest activation and the latest repolarization over the entire ventricles. Naturally, clinical corrected QT intervals are longer than those for simulated pseudo-ECG. Nevertheless, the pseudo-ECG QT interval for WT can be recalibrated to match normal clinical values (403 ms at 1 Hz). Using the recalibrated model, the het QT interval was 426 ms, similar to the corrected QT interval in the proband (430 ms, 1 Hz) under basal conditions. Importantly, I_{Ks} elimination (complete block), as in severe nonsilent LQT1, indeed caused QT prolongation consistent with LQT1 diagnosis (1 Hz basal QT ≥ 440 ms[1]).

The ORd does not represent gender or age differences; it was validated based on experiments from more than 100 undiseased human hearts, of which 56% were male of average age 41 ± 12 years.[11] Recent data showed K^+ current reduction in females compared with males.[22] Female gender may be an additional risk factor for patients with LQTS. The I_{Kr} block simulations presented relate to, but do not specifically account for, gender differences. Advanced age is also an LQT risk factor that can induce pathology of silent mutations.[23,24]

Conclusion

For the Q357R mutation, multiple insults to the repolarization reserve were needed to separate mutant from WT behavior. Yet, the separation was marginal. Simulations demonstrate that simple loss of channels at the membrane, not kinetics alterations, accounts for EAD generation in the silent mutation. The Q357R example admonishes that when considering arrhythmia-formation mechanisms in silent LQTS, it is important to apply quantitative analysis to determine whether the identified mutation, and not some external factor(s), was indeed the true cause of arrhythmia.

Supplementary Material

Refer to Web version on PubMed Central for supplementary material.

Acknowledgments

This work was supported by National Institutes of Health/National Heart, Lung, and Blood Institute grants R01-HL049054-19 and R01-HL033343-27033343-27 (to Y.R.), Fondation Leducq Award to the Alliance for CaMK Signaling in Heart Disease (to Y.R.), National Science Foundation grant CBET-0929633 (to Y.R.), and American Heart Association Predoctoral Fellowship 0815539G (to T.J.O.). Y. Rudy is the Fred Saigh Distinguished Professor at Washington University.

ABBREVIATIONS

AP	action potential
APD	action potential duration
CL	cycle length
EAD	early afterdepolarization
ECG	electrocardiogram
epi	epicardial
het	heterozygous
ISO	isoproterenol
LQT1	long QT syndrome type 1
LQTS	long QT syndrome
M	mid-myocardial
ORd	O'Hara Rudy dynamic human ventricular action potential model
WT	wild type

References

1. Roden DM. Clinical practice: long-QT syndrome. N Engl J Med. 2008; 358:169–176. [PubMed: 18184962]
2. Schwartz PJ, Stramba-Badiale M, Crotti L, et al. Prevalence of the congenital long-QT syndrome. Circulation. 2009; 120:1761–1767. [PubMed: 19841298]
3. Priori SG, Schwartz PJ, Napolitano C, et al. Risk stratification in the long-QT syndrome. N Engl J Med. 2003; 348:1866–1874. [PubMed: 12736279]
4. Schwartz PJ, Priori SG, Spazzolini C, et al. Genotype–phenotype correlation in the long-QT syndrome: gene-specific triggers for life-threatening arrhythmias. Circulation. 2001; 103:89–95. [PubMed: 11136691]
5. Roden DM, Yang T. Protecting the heart against arrhythmias: potassium current physiology and repolarization reserve. Circulation. 2005; 112:1376–1378. [PubMed: 16145010]
6. Wilde AA. Long QT syndrome: a double hit hurts more. Heart Rhythm. 2010; 7:1419–1420. [PubMed: 20601150]
7. Varro A, Papp JG. Low penetrance, subclinical congenital LQTS: concealed LQTS or silent LQTS? Cardiovasc Res. 2006; 70:404–406. [PubMed: 16678140]
8. Boulet IR, Raes AL, Ottschytsch N, Snyders DJ. Functional effects of a KCNQ1 mutation associated with the long QT syndrome. Cardiovasc Res. 2006; 70:466–474. [PubMed: 16564513]
9. Chen S, Zhang L, Bryant RM, et al. KCNQ1 mutations in patients with a family history of lethal cardiac arrhythmias and sudden death. Clin Genet. 2003; 63:273–282. [PubMed: 12702160]
10. O'Hara T, Virag L, Varro A, Rudy Y. Simulation of the undiseased human cardiac ventricular action potential: model formulation and experimental validation. PLoS Comput Biol. 2011; 7:e1002061. [PubMed: 21637795]
11. Gima K, Rudy Y. Ionic current basis of electrocardiographic waveforms: a model study. Circ Res. 2002; 90:889–896. [PubMed: 11988490]
12. Yan GX, Antzelevitch C. Cellular basis for the electrocardiographic J wave. Circulation. 1996; 93:372–379. [PubMed: 8548912]
13. Heijman J, Volders PG, Westra RL, Rudy Y. Local control of beta-adrenergic stimulation: effects on ventricular myocyte electrophysiology and Ca^{2+}-transient. J Mol Cell Cardiol. 2011; 50:863–871. [PubMed: 21345340]

14. Silva J, Rudy Y. Subunit interaction determines IKs participation in cardiac repolarization and repolarization reserve. Circulation. 2005; 112:1384–1391. [PubMed: 16129795]
15. Rocchetti M, Besana A, Gurrola GB, Possani LD, Zaza A. Rate dependency of delayed rectifier currents during the guinea-pig ventricular action potential. J Physiol. 2001; 534:721–732. [PubMed: 11483703]
16. Stengl M, Volders PG, Thomsen MB, Spatjens RL, Sipido KR, Vos MA. Accumulation of slowly activating delayed rectifier potassium current (IKs) in canine ventricular myocytes. J Physiol. 2003; 551:777–786. [PubMed: 12819301]
17. Nobrega AC, Araujo CG. Heart rate transient at the onset of active and passive dynamic exercise. Med Sci Sports Exerc. 1993; 25:37–41. [PubMed: 8423755]
18. Jost N, Virag L, Bitay M, et al. Restricting excessive cardiac action potential and QT prolongation: a vital role for IKs in human ventricular muscle. Circulation. 2005; 112:1392–1399. [PubMed: 16129791]
19. Guo D, Liu Q, Liu T, et al. Electrophysiological properties of HBI-3000: a new antiarrhythmic agent with multiple-channel blocking properties in human ventricular myocytes. J Cardiovasc Pharmacol. 2011; 57:79–85. [PubMed: 20980921]
20. Wu D, Delaloye K, Zaydman MA, Nekouzadeh A, Rudy Y, Cui J. State-dependent electrostatic interactions of S4 arginines with E1 in S2 during Kv7.1 activation. J Gen Physiol. 2010; 135:595–606. [PubMed: 20479111]
21. Marx SO, Kurokawa J, Reiken S, et al. Requirement of a macromolecular signaling complex for beta-adrenergic receptor modulation of the KCNQ1–KCNE1 potassium channel. Science. 2002; 295:496–499. [PubMed: 11799244]
22. Gaborit N, Varro A, Le Bouter S, et al. Gender-related differences in ion-channel and transporter subunit expression in non-diseased human hearts. J Mol Cell Cardiol. 2010; 49:639–646. [PubMed: 20600101]
23. Goldenberg I, Moss AJ, Bradley J, et al. Long-QT syndrome after age 40. Circulation. 2008; 117:2192–2201. [PubMed: 18427134]
24. Nishio Y, Makiyama T, Itoh H, et al. D85N, a KCNE1 polymorphism, is a disease-causing gene variant in long QT syndrome. J Am Coll Cardiol. 2009; 54:812–819. [PubMed: 19695459]

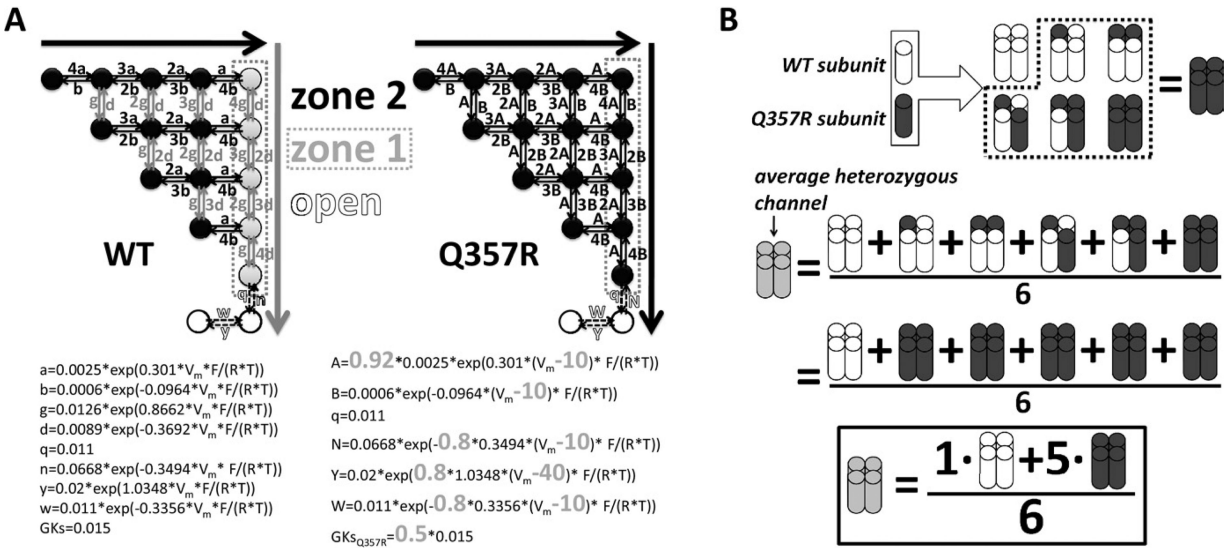

Figure 1.

Markov I_{Ks}. **A:** Schematic diagrams and transition rate equations. The WT model is on the left; Q357R is on the right. Equations are below the diagrams (differences from WT are in large bold gray type). WT model activation, as proposed by Silva and Rudy,[14] represents 2 voltage sensor transitions. First transitions are from left to right (large black arrow) and second transitions are from top to bottom (large gray arrow). Channel kinetic states are divided into 2 zones. Different from WT where zone 1 (gray circles) transitions are rapid, for Q357R these transitions are the same as the slower zone 2 (black circles) transitions. **B:** WT (white) and Q357R (black) subunits combine to form 6 tetramer permutations in the heterozygous (het) case (gray). The model considers that the mutation was dominant negative. Thus, the behavior of the average het channel is the average behavior of the permutations: het = (1 × WT + 5 × Q357R)/6. WT = wild type.

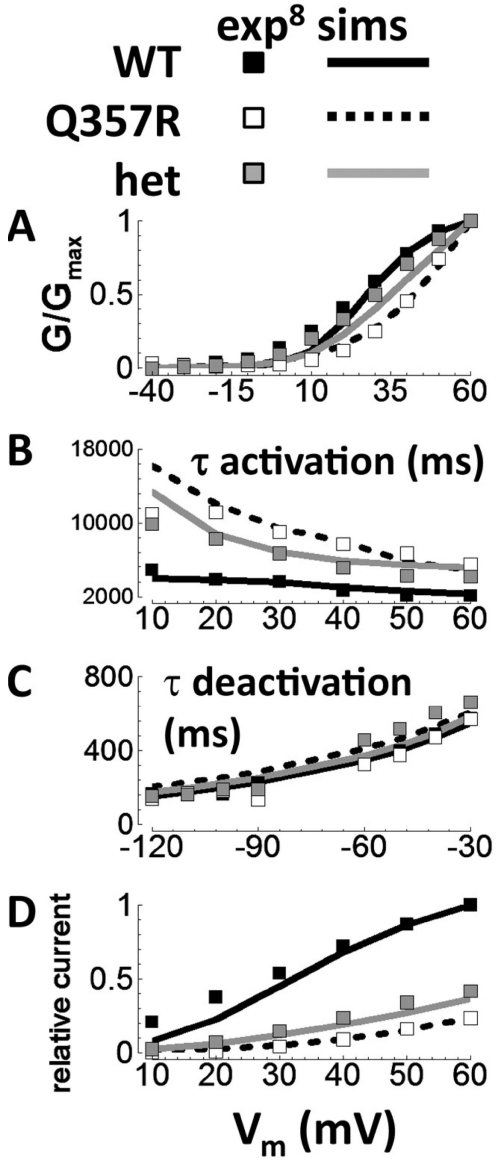

Figure 2.

Validation for WT, Q357R, and het I_{Ks}. Experiments are from Boulet et al[8] (squares: WT is black, Q357R is white, and het is gray). **A:** Steady-state activation of tail currents. **B:** Time constant for step current activation. **C:** Time constant for deactivation. **D:** Relative current, after 5-second steps to the potentials shown along the abscissa. Simulated protocols were the same as those used in Boulet experiments. Exp, experiments; sims, simulations. het = heterozygous; WT = wild type.

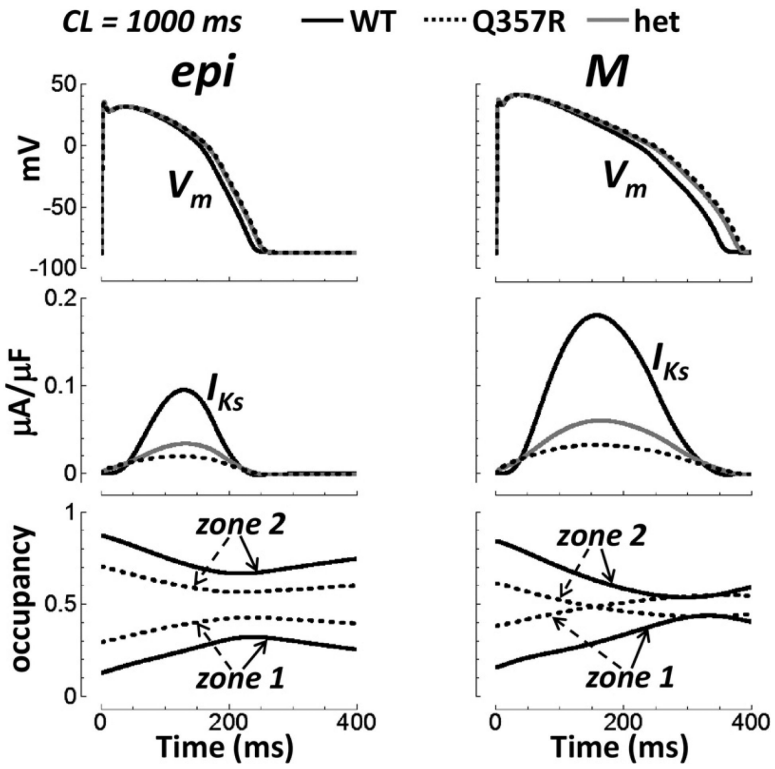

Figure 3.

Basal conditions and normal pacing rate (CL = 1000 ms). Epi (left) versus M cell (right) under basal conditions (no isoproterenol). The top row shows APs. I_{Ks} is the middle row. Closed state zone occupancy is below. Time = 0 is the start of the final paced AP. AP = action potential; CL = cycle length; epi = epicardial; het = heterozygous; M = mid-myocardial; WT = wild type.

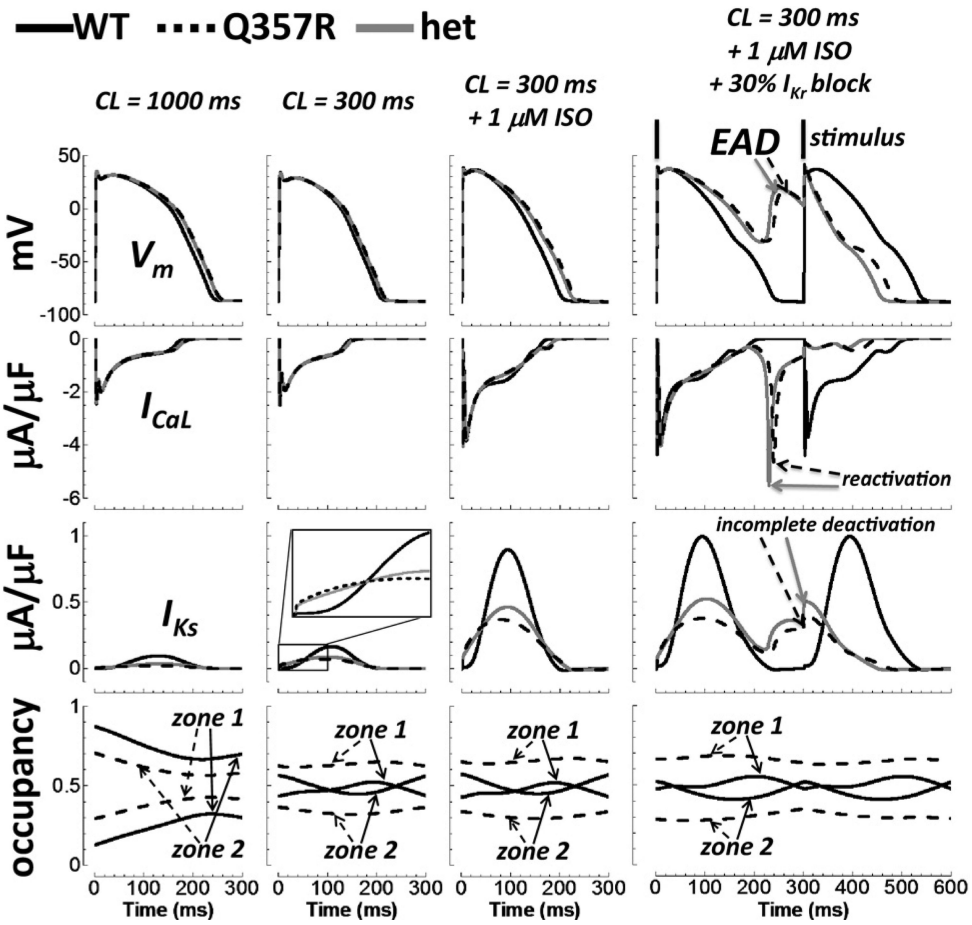

Figure 4.

Effect of multiple insults on the AP in epi cells. Descending rows show the AP, I_{CaL}, I_{Ks}, and closed state zone occupancy. Columns, from left to right, show normal pacing under basal conditions, fast pacing under basal conditions, fast pacing with application of ISO, and 30% I_{Kr} block in addition to fast pacing and ISO. EADs in the rightmost column (top row, arrows) were caused by I_{CaL} reactivation (second row, arrows) due to prolongation of AP plateau (deficient I_{Ks}, third row). The AP following the EAD is short because of the residual activation of I_{Ks} (incomplete deactivation, arrows). AP = action potential; CL = cycle length; EAD = early afterdepolarization; epi = epicardial; ISO = isoproterenol; het = heterozygous; WT = wild type.

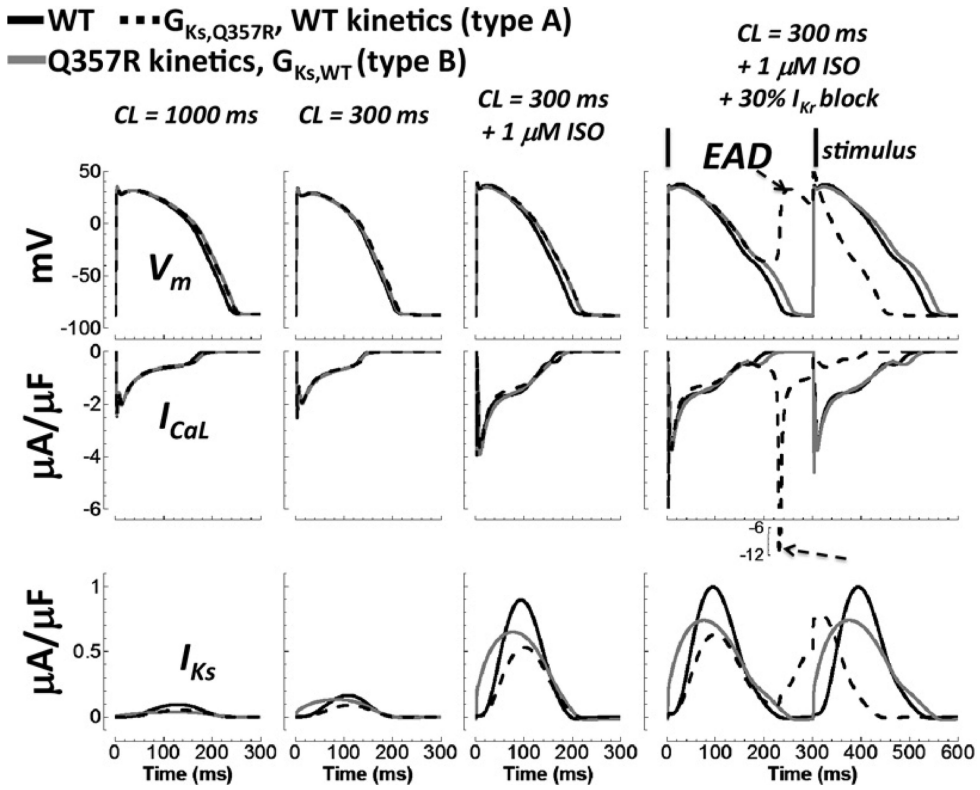

Figure 5.

Effect of reduced conductance versus kinetic changes in the silent mutation. WT, WT with Q357R conductance (mutant type A), and WT with Q357R kinetics (mutant type B) are black, dashed black, and gray lines, respectively. Descending rows show the AP, I_{CaL}, and I_{Ks}. The four columns, from left to right, show the cases for normal pacing under basal conditions, fast pacing under basal conditions, fast pacing with application of ISO, and 30% I_{Kr} block in addition to fast pacing and ISO. Insults of fast pacing with ISO caused AP prolongation relative to WT. With addition of I_{Kr} reduction, kinetic changes alone did not cause EAD formation, but reduced conductance alone did (arrows, rightmost column). AP = action potential; CL = cycle length; EAD = early afterdepolarization; ISO = isoproterenol; WT = wild type.

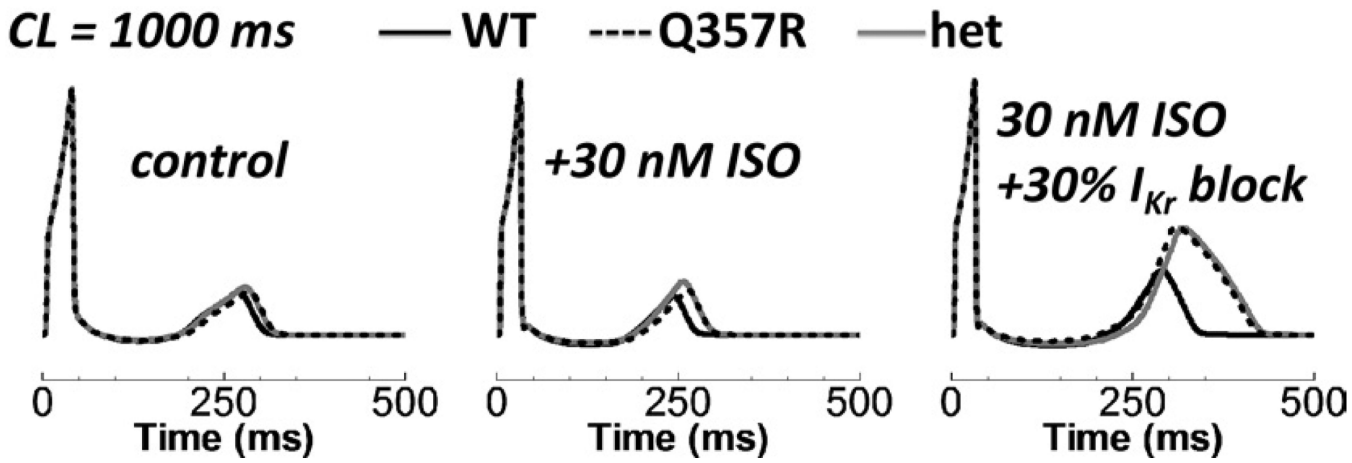

Figure 6.

Effects of ISO and I_{Kr} reduction on the pseudo-ECG. The simulated pseudo-ECG is plotted by using a shared, normative scale. On the left, middle, and right, the cases of control, ISO, and 30% I_{Kr} block plus ISO are shown. CL = cycle length; ECG = electrocardiogram; het = heterozygous; ISO = isoproterenol; WT = wild type.

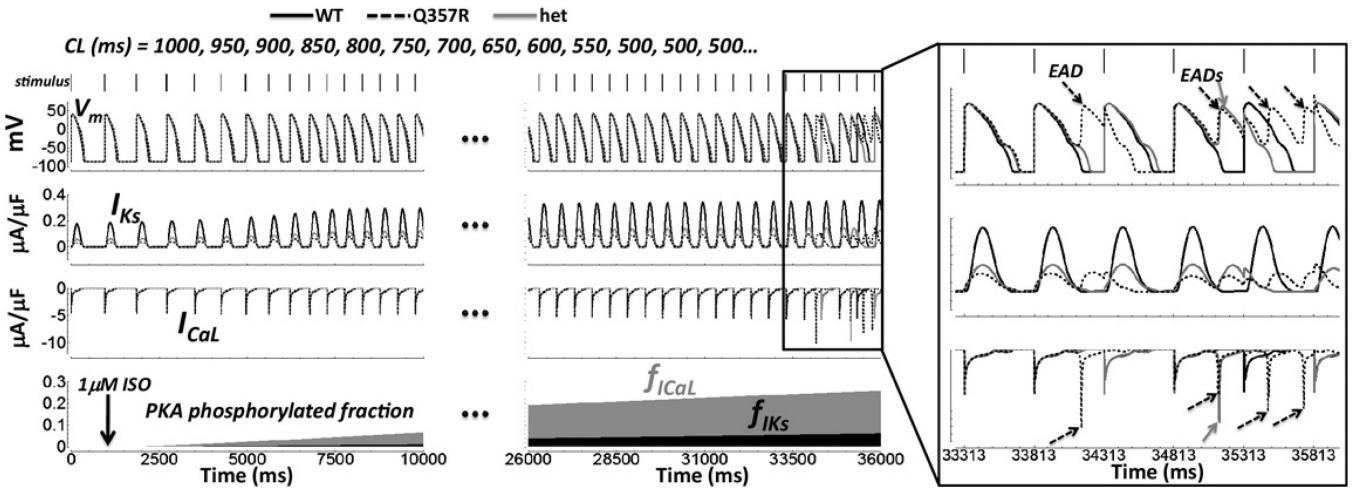

Figure 7.

Exercise onset. Simulations are in M cells. Shown from top to bottom: APs, I_{Ks}, I_{CaL}, and fraction of I_{CaL} (f_{ICaL}, gray) and I_{Ks} (f_{IKs}, black) channels phosphorylated by PKA. Bars along the top show the accelerating stimulus delivery. An ISO bolus of 1 μM was applied at t = 1000 ms (arrow in bottom panel). Time axis is broken (dots), skipping an uneventful midsection. The box on the far right shows the final paced beats on an expanded time scale. Arrows show EADs caused by I_{CaL} reactivation. AP, action potential; CL, cycle length; EAD, early afterdepolarization; het, heterozygous; ISO, isoproterenol; PKA, protein kinase A; WT, wild type.